DCT-Based Characterization of Milk Products Using Diffuse Reflectance Images

Sara Sharifzadeh, Jacob L. Skytte, Line H. Clemmensen, Bjarne K. Ersb¿ll
Department of the Applied Mathematics and Computer Science
Technical University of Denmark
Copenhagen, Denmark
{sarash, jlsk, lkhc, bker}@dtu.dk

Abstract— **We propose to use the two-dimensional Discrete Cosine Transform (DCT) for decomposition of diffuse reflectance images of laser illumination on milk products in different wavelengths. Based on the prior knowledge about the characteristics of the images, the initial feature vectors are formed at each wavelength. The low order DCT coefficients are used to quantify the optical properties. In addition, the entropy information of the higher order DCT coefficients is used to include the illumination interference effects near the incident point. The discrimination powers of the features are computed and used to do wavelength and feature selection. Using the selected features of just one band, we could characterize and discriminate eight different milk products. Comparing this result with the current characterization method based of a fitted log-log linear model, shows that the proposed method can discriminate milk from yogurt products better.**

Keywords—discrete cosine transform; entropy; diffuse reflectance image; discrimination power

I. INTRODUCTION

The Discrete Cosine Transform (DCT) is an appropriate transformation in the field of signal processing. It was first introduced in [1] to be used in the image processing area for the purpose of feature selection. It has excellent decorrelation properties as well as energy compaction. In addition, it decomposes the spatial frequency of an image in terms of various cosines transforms. Some of its application areas are image and speech compression [2, 3], speech recognition [4, 5] and medical imaging [6].

In this paper, the DCT is employed for decomposition of diffuse reflectance images. These images are obtained by illumination of a hyperspectral coherent laser (460-1000 nm) into the surface of eight different milk products. This vision system has been introduced recently for inspection of the structure of food items [7, 8]. It is applicable for homogenous products where particle size and shape are important parameters. The main idea is to use the diffusion effects, which are known to be correlated to the microstructure, for characterization of the structural composition of food items [9, 10].

On the other hand, research findings in the field of food quality control have demonstrated a correlation between the texture, chemical and physical properties of food items with their microstructure characteristics [11, 12].

Considering these sequential relationships from the optical level to the quality level, it is possible to build an automatic light-based system as a measuring tool, for monitoring the quality of dairies along the production line and avoid unwanted structures during the process.

Therefore, finding an efficient method for characterization of the hyperspectral images into key discriminative features obtained from a minimum number of bands is of special concern in this field. The reduction in the number of required wavelengths will assist to simplify the laser set-up and make the overall system simpler and cost effective.

According to the characteristics of the milk products e.g. fat or viscosity, we can observe different visual effects in the hyperspectral images. The main optical feature is the low frequency light diffusion emanating from the incident point that has the highest intensity in the image as can be seen in Fig. 1(a). Another important effect is a high frequency speckle pattern caused by interference of coherent light due to surface irregularities [13]. It is shown in Fig. 1(b) by zooming in around the center point. These effects vary in different products according to their molecular composition and thus reflectance and scattering properties of light.

The current characterization technique for these images uses a narrow band of pixels of the scattering profile including the scattering center [7, 8, and 14]. A double logarithm transformation is applied on the original profile to form this image. Therefore, the extracted line of intensities is called the log-log model. The resulting profile includes a slope and an intercept containing the subsurface and surface information respectively. This method only considers the low frequency information in the image.

In this paper, we propose to apply a DCT transform on the double logarithm of the entire diffuse reflectance image to decompose the low frequency diffusion effect as well as the high frequency speckle patterns. DCT can decorrelate the highly correlated information in these images. It decomposes the low frequency diffusion effects and high frequency speckle effects into low and high order coefficients that could be quantified easier. Finally, due to the high compression level in the DCT domain, the number of discriminative features is

This work was financed by the Centre for Imaging Food Quality project which is funded by the Danish Council for Strategic Research (contract no 09-067039) within the Program Commission on Health, Food and Welfare.

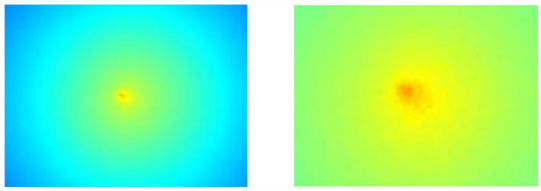

(a) (b)

Figure 1. (a) A log-log transformed diffuse reflectance image of yogurt showing the low frequency diffusion effect at the center. (b) The zoomed image showing the high frequency speckle noise around the incident point caused by the destructive interference of light to the rough surface of fermented milk.

reduced. In order to form an initial set of features for each image of each wavelength, we combine those of both low and high frequency effects. The low order DCT coefficients are considered to characterize the optical properties. The entropy information of the high order coefficients are used to characterize the speckle effect based on an approach that will be explained in section 3.

In the next step, the discrimination power analysis (DPA) introduced in [15], is employed as a selection criterion on the initial set of features for both wavelength and feature selection. It is a more careful method in terms of discrimination than the conventional zigzag or zonal masking for DCT coefficient selection. Especially, that is in our work, both the low and high order features are important. Using the final selected features of one proper wavelength, we could characterize and discriminate the eight different products.

The proposed method is compared to the previous profile based characterization method including low frequency information and the results show that in addition to the more discrimination power of the proposed method (including both the low and high frequency information), it can separate the milk class products from the yogurt class better.

The rest of this paper is organized as follows. In section II, the data is described. Section III presents the characterization of the diffuse reflectance images. In section IV, feature selection and discrimination is explained. The experimental results are shown in section V. Finally, there is a conclusion for this paper.

II. DATA DESCRIPTION

The data set consists of spectral diffuse reflectance images (1200×1600 pixel) of eight commercial dairy products including milk and yogurt categories. Table I. shows their names and fat levels. L, M and H stand for low, medium and high. The CH and CU are extracted from the commercial name of the products. In each category, there are products with different fat levels and viscosities. In the yogurt category, there are two different products with similar fat levels. The yogurt products differ from each other not only in terms of the fat, but also according to the applied fermentation processes. In this paper, we are not interested in predicting these kinds of features. Instead, we would like to characterize the products diffuse reflectance profiles and then discriminate them using their optical features. In fact, the optical characteristics represent

TABLE I. THE EIGHT MILK PRODUCTS AND THEIR FAT LEVELS

Product Type	*Yogurt*					*Milk*		
Short Names	*L*	*M*	*H*	*CH*	*CU*	*L*	*M*	*H*
Fat Level	0.5	1.5	3.5	0.1	1.5	0.5	1.5	3.5

the chemical, physical and structural differences between the products. For each product, there are five samples in the data set. Thus, there are 40 samples available in total. The laser was illuminated in 55 wavelengths (460-1000 nm).

III. CHARACTERIZATION OF THE IMAGES

As mentioned in section I there are two important features in the diffuse reflectance images that can be used for characterization of these images; the low frequency light diffusion effect and the high frequency speckle effect.

The light diffusion effect shows the spatial intensity distribution due to the absorption and scattering of the light. It is mostly dependent on the microstructural characteristics of the subsurface such as particle size distribution.

The speckle effect is caused by the interference of light at the surface. It can be seen as a measure of surface roughness. In a fermented milk product like yogurt, the surface roughness is higher than milk due to the increase in viscosity of the material after the fermentation process. Hence, it could be used as a measure for distinguishing milk from yogurt. Fig. 2 shows in the top row, two diffusion images of a medium-fat milk sample (M-M) and a high-fat yogurt (Y-H). The images are zoomed around the incident point. The difference in both low frequency diffusion effect and the high frequency speckle noise effect is clear between the two images.

A. DCT Transform

Two dimensional DCT transform is applied to the diffuse reflectance images of each sample product at each wavelength. This yields 40×55 DCT matrixes of size 1200×1600. In the second row of Fig. 2, the corresponding 400×400 DCT coefficients from the top-left DCT matrix of the above images are illustrated. The difference in the higher order DCT coefficients represents the speckle effect that was seen in the spatial domain as well. However, it is not easy to distinguish the difference in low order DCT coefficients that represent the diffusion effect.

According to these observations, choosing the DCT coefficients in a conventional zigzag or zonal low order masking alone, is not a good choice. That is due to the large number of DCT coefficients in a wide span of low and high frequencies that describe the scattering and speckle effect. To demonstrate this issue, a 400×400 sub-volume of DCT coefficients from the top-left of the DCT matrix is considered for all the samples of all classes. For ease of visualization, they are sorted and just the logarithm of the 50 highest are illustrated in Fig. 3(a). It is difficult to distinguish all the products. In addition, they are transformed into the PCA domain and the first two PCs are shown in Fig. 3(b). In both images, just a few products can be distinguished from each other and the other classes. It is not easy to distinguish most fermented products and the high-fat

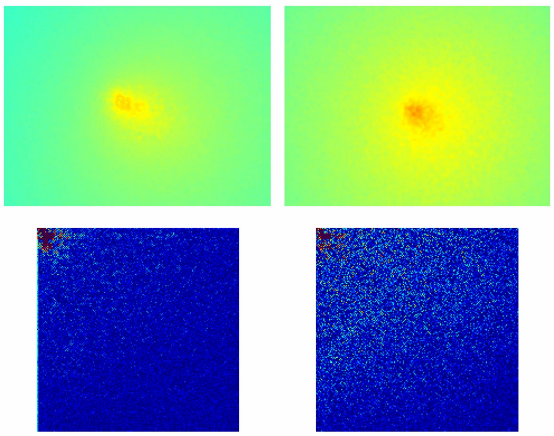

Figure 2. (Top) left and right, the zoomed diffuse reflectance images of milk-M (1.5) and yogurt-H (3.5) respectively. (Down) their corresponding 400×400 top-left DCT coefficients from the DCT matrix

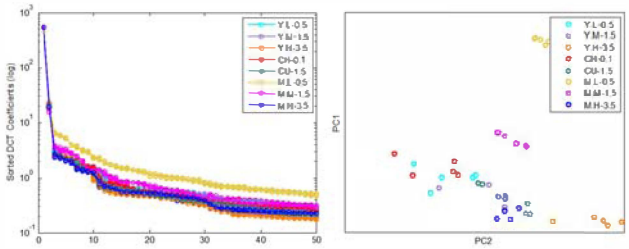

(a) (b)

Figure 3. The first 50 highest DCT coefficients of all the samples of the 8 products: (a) in original domain (b) in PCA space using the first two PCs.

milk from each other. This is because; the higher values of the DCT coefficients only carry the information about the diffusion effect and that is not enough for discrimination. In order to include the speckle effect, we propose to use the entropy of the DCT coefficients which will be explained in the following section.

B. Entropy

The high frequency DCT coefficients that contain information about the speckle effect result in an increase in the entropy of the sub-volumes of the DCT matrix that include them. For example, in the two 400×400 sub-volumes that are shown at the bottom of Fig. 2, the entropies are 1.55 and 2.02 from left to right respectively. Starting from the top-left corner of a DCT matrix, we considered an $n \times m$ sub-volume and calculated the entropy repeatedly, while continuously increasing the n and m values as illustrated in Fig. 4(a). The resulting entropy profile is shown in Fig. 4(b). It shows that, as the size of the volume increases, the entropy also increases up to some point and then, decreases due to the uniform values of the DCT coefficients in higher frequencies. Since the speckle effect that characterizes the surface roughness enhances the higher order DCT coefficients, the maximum entropy should describe the speckle effect for each sample. By forming such entropy profile for the eight products, we found that it can characterize their speckle effect uniquely. Therefore, the low entropies before the peak point can be considered as the diffusion effect so that, their corresponding sub-volumes include mostly the DCT coefficients describing the diffusion effect. On the other hand, the right side of the peak point includes the higher order DCT coefficients that describe the diffusion effect. To verify this further, we isolated the low order diffusion effect DCT coefficients using the index of the peak point that is 52 in Fig. 4(b). Then, an inverse DCT transform is applied to this 52×52 DCT sub-volume. Comparison of the result with the original diffuse reflectance image shows the removal of the speckle effect, as shown in Fig. 4(c, d).

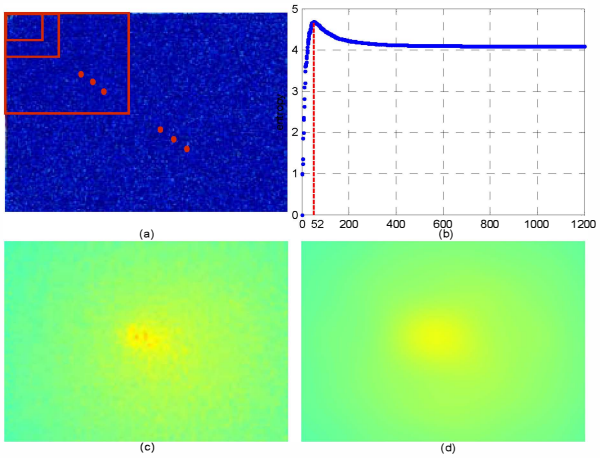

Figure 4. (a) The sequential entropy calculation on increasing sub-volumes of the DCT matrix. (b) The resulting entropy profile. (c) The zoomed original diffusion image around the incident point. (d) The diffusion image obtained by the inverse DCT transform of the 52×52 lower order sub-volume of the DCT matrix.

C. Forming the Initial Feature Set

According to the discovered points, the right side of the entropy profile was considered for characterization of the speckle effect. The mean, the standard deviation and the maximum value, of this part of the profile were considered as the candidate speckle effect features. By looking to the entropy profiles of the eight products, it was found that in average, the maximum entropy occurs around a 50×50 sub-volume. Regarding to its variation in different products and also considering a softer threshold for separation of the DCT coefficients of the diffusion and speckle effects, a 20×20 sub-volume of low order DCT coefficients was considered. They form a 400 length vector as the candidate feature for the light diffusion effect.

The final initial set of features for each wavelength image was formed by concatenating the three candidate features of the speckle effect with the 400 of the diffusion effect.

D. Feature Forming based on log-log model

In order to form the features based on log-log model, at each wavelength, a narrow diagonal band (around 10 pixels width) including the scattering center was considered in the double logarithm of the diffuse reflectance image as shown in Fig. 5 (a). The orientation of the line was chosen in a way to consider as much as possible, higher number of pixels along the path through the center. Then, it was averaged over the pixels.

Since this diagonal line is symmetric, just half of that was considered. The resulting averaged profile includes an intercept from the peak and a slope as shown in Fig. 5(b). These two features were used to characterize the image. For more information, we refer to [7, 8].

IV. Feature Selection and Discrimination

The length of the formed initial set of features (403) per band, regarding the total number of samples of all classes (40) is quite high. Therefore, it is better to select a subset of them according to their ability for characterization and discrimination of different products. Besides that, there are 55 bands per sample and as mentioned earlier, we are interested to reduce the number of wavelengths to simplify the laser set-up. Therefore a strategy should also be taken into account to sort the discrimination ability of different wavelengths and select one or a few number of them.

Since majority of the features are the decorrelated DCT coefficients, it is not necessary to decorrelate them by a transformation into an orthogonal space. Inspired by the approach in [15], we employ the DPA introduced in that work. The main idea behind this data-dependent approach is that, all of the DCT coefficients do not have the same discrimination power (DP). In other words, some of them can discriminate the classes better than the others. It is different from other similar approaches such as PCA and LDA, in the sense that it does not utilize the between- and within- class variances by a transformation to maximizes the discrimination of the features in the transformed domain. It searches for the best discriminant features in the original domain. In case of decorrelated features such as DCT coefficients it is an appropriate approach for ranking the features and choosing a sub-set of them. The calculation of DPA will be explained step by step in the following.

Assuming that we have C classes with the N_c number of data points and $P=403$ features in each class, the DP_j of each feature f_j $(j = 1, 2, \dots, 403)$ is calculated as follows:

1. The mean and variance of each class is calculated for that feature (f_j): $m_{jc} = \frac{1}{N_c}\sum_{n=1}^{N_c} f_{nj}, c = 1, 2, \dots, C$, $v_{jc} = \sum_{n=1}^{N_c}(f_{nj} - m_{jc})^2, c = 1, 2, \dots, C$
2. The variance of all classes are averaged: $V_j^w = \frac{1}{C}\sum_{c=1}^{C} v_{jc}$
   The mean and variance of all training samples are calculated for f_j : $M_j = \frac{1}{C \times N_c}\sum_{c=1}^{C}\sum_{n=1}^{N_c} f_{nj}$, $V_j^B = \sum_{c=1}^{C}\sum_{n=1}^{N_c}(f_{nj} - M_j)^2$
3. The DP can be estimate as $DP_j = \frac{V_j^B}{V_j^w}$

It is mentioned in [15] that DPA can be used as a stand-alone feature reduction algorithm. Since we need to do both band and feature selection, a sequential strategy is taken into account as shown in Fig. 6.

A. Preparation of Training and Test Sets

In order to maintain the training and test sets from the few data points, one sample of each class was considered as the unseen test data and the rest were assigned to the training set. Therefore, the two sets were formed as $test_{8\times403\times55}$, $train_{32\times403\times55}$. Then, leave one out cross validation (LOOCV) was used on the training data set for both wavelength selection and feature selection steps. LOOCV is used for generalization and to avoid over-fitting as much as possible [16]. However, due to the limited training data points, this could not be achieved completely.

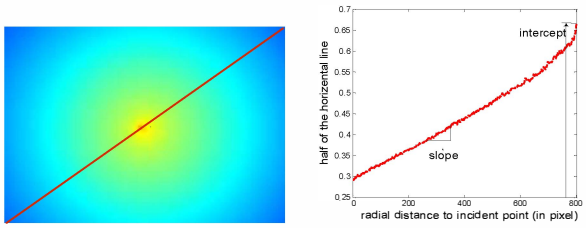

(a) (b)

Figure 5. (a) Symmetric narrow band of pixels crossing the incident point in the double logarithm diffuse reflectance image. (b) Half of the band is averaged and the slope and intercept from the peak are shown.

B. Wavelength Selection

The band selection algorithm is as follows:

1. At each iterations of LOOCV, sum of the DPs of all 403 training features are calculated at each wavelength $w = 1,2, \dots ,55$; $SUM_{32\times55}$.
2. The sum of DPs, $SUM_{32\times55}$ is averaged over the 32 iterations; $Average\_SUM_{1\times55}$.
3. The best band is the one with the highest average discrimination power.

This algorithm was also used for wavelength selection of the log-log model.

C. Feature Selection for The Selected Band

The use of just one band is a significant reduction in the number of features, since there are 403 initial features per wavelength. In order to select the most discriminative features of the selected band, these steps are followed:

1. The DPs of the features in the selected band are sorted for each of the 32 LOOCV iterations in descending order. Then, the corresponding features to the first top five DPs at each iteration are kept in a list; $list_{32\times5}$
2. The densities of the N_u unique features in this list are calculated. $Density_{1\times N_u}$
3. According to these densities, the features that were among the top five features almost in all 32 LOOCV iterations are selected as the final features.

The number five in the above explained procedure was chosen empirically by looking to the sorted features and also for the aim of selecting a limit number of features. Interestingly, we observed in all the iterations, the first three features were from distinct low frequency DCT coefficients representing the light diffusion effect and one of the last two was the mean value of the speckle effect from the entropy profile shown in Fig.4 (b).

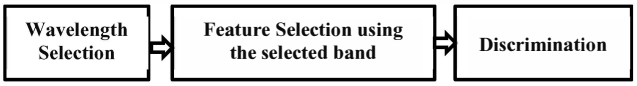

Figure. 6 The three steps of the sequential strategy

D. Discrimination

In order to evaluate the proposed characterization approach and compare it with the existing log-log method, the training and test data are visualized on the same plot. Besides that, the discrimination power of the two methods is numerically measured by sum of the features' DPs as well as the maximum Rayleigh quotient term [16]:

$$max \frac{a^T Ba}{a^T Wa} \quad (1)$$

Where, B and W are the between- and within-class covariance matrixes and a is the Eigen vector of the generalized Eigenvalue problem, $\det(B - \lambda W) = 0$. In order to maximize (1), the Eigen vector a_1 corresponding to the highest Eigen value λ_1 should be used. In addition, the support vector machine (SVM) classifier with a linear kernel is used [17] and the average LOOCV results and unseen test results are compared for the two methods.

V. Results and Discussion

First, the results of the proposed method in DCT domain will be shown. Then, the log-log model results will be presented. Finally, there is a discussion.

A. Characterisation Results in DCT Domain

As explained in the previous section, both the band selection and feature selection were performed using LOOCV on the training data. Fig. 7(a) shows the average sum of the DPs for the 55 bands. According to this plot, the highest sum of DPs obtained for band 38 (830 nm).

By sorting the features' DPs in this band, a list of features corresponding to the top five DPs were formed for the 32 LOOCV iterations. There were eight unique features in the list. Fig. 7(b) shows the densities of the unique features in the list. As can be seen, three features were among the top features in all 32 iterations. They are the low order DCT coefficients showing the light diffusion effect. Their location in the DCT matrix is represented in Fig. 8. In addition, the feature number one that represents the mean entropy of the speckle effect was among the top five features in 31 of the iterations. These four features were selected as the final features, for characterizing the samples.

In order to visualize the ability of the speckle effect features to separate the two groups of yogurt products and milk, a 3D visualization of the mean, standard deviation and maximum features (1, 2, 3 in Fig. 8) is represented in Fig. 9(a). The results show that these features are capable to perform the separation accurately for both training and test data. In addition to this between group separations, we can also observe a trend for within group separation according to the fat level. Fig 9(b) shows the 3D visualization of the three diffusion effect features (4, 6, 44 in Fig. 8). As can be seen, they fail to separate the high-fat milk sample (M-H) and the medium-fat yogurt (Y-M). Since the visualization of the 4D selected features is impossible, three of them (1, 4, 6) are chosen and visualized in Fig. 9(c). Even in absence of one of them, we can see the successful separation of all the classes and also the two groups of milk and yogurt. Finally, the four features are transformed into the orthogonal PCA space and the first two PCs are shown in Fig. 9(d). Besides the successful discrimination, we can observe that the PC1 represents the variation from yogurt to milk group, while PC2 shows the change in fat content.

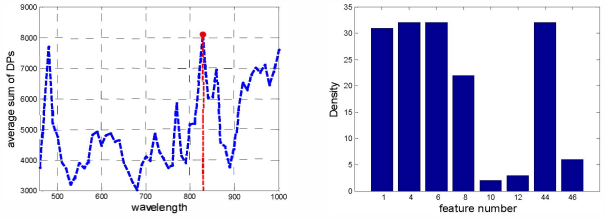

(a) (b)

Figure 7. (a) Average sum of DPs over the 32 LOOCV iterations for the 55 bands. (b) Density of the 8 unique features found among the top five discriminative features in the list over the 32 iterations. The horizontal axis shows the features' number among the 403 features.

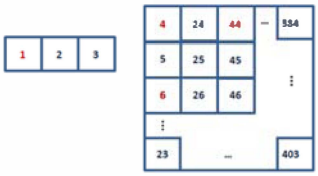

Figure 8. The 1, 2 and 3 are the mean, standard deviation and maximum of the entropy profile of the speckle effect. The 400 low order DCT features' numbers start from 4.

B. Characterisation Results Using the log-log Model

The same wavelength selection strategy based on sum of discrimination powers were used for band selection for log-log model dataset. Fig. 10 shows the 2D visualization of the slope and intercepts features in original as well as PCA space. In both spaces, the two features group the samples only according to their fat level, while there is no trend to separate the milk group from the yogurt group. For example the high fat milk (M-H) and the medium fat yogurt (Y-M) have close overlap which may make the discrimination difficult.

C. Discussion

According to the visualized results, the combination of the speckle effect (high frequency) and diffusion effect (low frequency) features in DCT domain shows to be a promising way of characterizing the diffuse reflectance images. The statistical analyses results are presented in Table II. Although both methods could discriminate the single test samples of all classes, the average LOOCV classification performance shows that the proposed method can work better. However, the statistical models suffer from the over-fitting due to the limited number of samples. The table results show that, the DCT domain features are capable to characterize the images better in terms of discrimination power and Rayleigh criteria than the

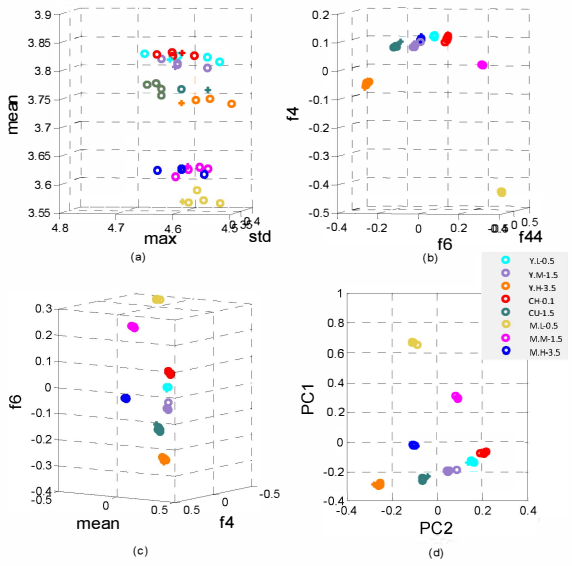

Figure 9. (a) 3D visualization of speckle effect features (b) 3D visualization of the three diffusion effect selected features (c) 3D visualization of speckle and diffusion selected features (d) 2D plot in PCA space using the first two PCs. The ÔoÕshows a training sample and Ô+Õshows a test sample.

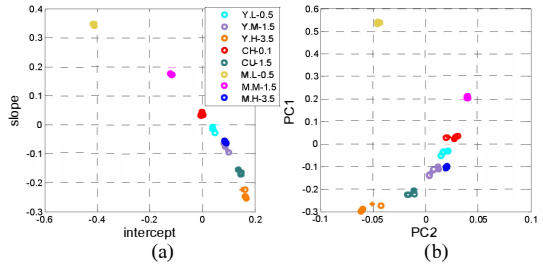

Figure 10. 2D visualization of the log-log model features (a) in original space (b) in PCA space.

log-log model features. Besides that, considering the plots in Fig. 9 and Fig. 10, they are capable to reduce the overlap between classes and separate the products not only according to their fat level, but also according to their category (milk-yogurt). That is obtained by employing the ability of DCT transform in frequency decomposition and combining the high and low frequency information of the images. When only the analysis of the diffusion effect is needed, this frequency-decomposed information can be used to exclude the speckle effect as shown in Fig. 4(d), using the inverse DCT transform.

VI. CONCLUSION

In this paper, a DCT-based characterization method is introduced for diffuse reflectance images. These images result from illumination of a narrow laser beam in different wavelengths into eight different dairies. They were milks and yogurts of different types and fat levels. The low order DCT coefficient were used to characterize the low frequency light diffusion effect and the entropy information of higher order DCT coefficients were used to characterize the speckle effect in the images. The discrimination power criterion was used to reduce

TABLE II. THE DISCRIMINATION RESULTS

	Av. SVM Perf. of LOOCV	*SVM Test Perf.*	*Sum of DPs of the selected features*	*Rayleigh criteria*
DCT	100%	100%	2460.3	5850.6
Log-Log Model	96.87%	100%	1815.1	79.60

the number of wavelength and to select the features. The existing characterization method based on a linear log-log model can only separate the products according to their fat levels, but the proposed method can discriminate them based on both their category (milk-yogurt) and fat level. It also improves the discrimination and removes the overlap between the classes.

REFERENCES

[1] N. Ahmed, T. Natarajan, K. R. Rao, ÒDiscrete cosine transform,ÓIEEE Transactions on Computers, vol. C-32, pp. 90-93, 1974.

[2] R. C., Gonzalez, R. E. Woods, ÒDigital Image Processing,ÓNew Jersey, USA: Prentice Hall, 2001.

[3] M. Arjona Ramírez and M. Minami, "Low bit rate speech coding," in Wiley Encyclopedia of Telecommunications, J. G. Proakis, Ed., New York: Wiley, vol. 3, pp. 1299-1308, 2003.

[4] J. Bouvrie, T. Ezzat, T. Poggio, "Localized spectro-temporal cepstral analysis of speech,Ó ICASSP, pp. 4733-4736, 2008.

[5] S. Sharifzadeh, J. Serrano, J. Carrabina, ÒSpectro-temporal analysis of speech for Spanish phoneme recognition,ÓIWSSIP, pp. 548-551, 2012.

[6] J.C. Fu, S.K. Lee, S.T.C. Wong, J.Y. Yeh, A.H. Wang, H.K. Wu,Ó Image segmentation feature selection and pattern classification for mammographic microcalcifications,Ó Computerized Medical Imaging and Graphics, vol. 29, pp. 419Ð429, 2005.

[7] O. H. A. Nielsen, A. L. Dahl, R. Larsen, F. M¿ller, F. D. Nielsen, C. L. Thomsen, H. Aan³s, J. M. Carstensen, ÓSupercontinuum light sources for hyperspectral subsurface laser scattering,ÓSCIA, pp. 327-337, 2011.

[8] O. H. A. Nielsen, A. L. Dahl, R. Larsen, F. M¿ller, F. D. Nielsen, C. L. Thomsen, H. Aan³s, J. M. Carstensen, ÓIn depth analysis of food structures,ÓScandinavian workshop on imaging food quality, pp. 29-34, 2011.

[9] F. Martelli, S. Del Bianco, A. Ismaelli, G. Zaccanti, ÒLight Propagation through Biological Tissue,ÓBellingham, Washington, USA: SPIE Press, 2010.

[10] M. J. Mateo, D. J. OÕCallaghan, C. D. Everard, M. Castillo, F. A. Payne, C. P. OÕDonnell, ÓEvaluation of on-line optical sensing techniques for monitoring curd moisture content and solids in whey during syneresis,Ó Food Research International, vol. 43, pp. 177Ð182, 2010.

[11] M. Bourne, ÒFood texture and viscosity: concept and measurement,Ó Academic Press, 2002.

[12] J. Aguilera, ÒWhy food microstructure?,ÓJournal of Food Engineering vol. 67, pp. 3Ð11, 2005.

[13] J.W. Goodman, ÒSpeckle Phenomena in Optics: Theory and Applications,ÓUSA, Roberts and Company Publishers, 2006.

[14] S. Sharifzadeh, J. L. Skytte, O. H. Nielsen, B. K. Ersb¿ll, L. H. Clemmensen, ÓRegression and sparse regression methods for viscosity estimation of acid milk from itÕs SLS features,Ó IWSSIP, pp. 58-61, 2012.

[15] S. Dabbaghchian , M. P. Ghaemmaghami, A. Aghagolzadeh, ÒFeature extraction using discrete cosine transform and discrimination power analysis with a face recognition technology,ÓPattern Recognition, vol. 43, pp. 1431Ð1440, 2010.

[16] R. Tibshirani, T. Hastie, J. Friedman, ÒThe Elements of Statistical Learning,ÓSpringer, 2001.

[17] Ch. Ch. Chang, Ch. J.Lin, ÒLIBSVM: a library for support vector machines,ÓACM Transactions on Intelligent Systems and Technology, vol. 2, pp. 27:1--27:27, 2011.